Progress in PHOTOVOLTAICS

PROGRESS IN PHOTOVOLTAICS: RESEARCH AND APPLICATIONS
Prog. Photovolt: Res. Appl. 2013; **21**:1507–1513
Published online 6 June 2012 in Wiley Online Library (wileyonlinelibrary.com). DOI: 10.1002/pip.2222

SHORT COMMUNICATION

Enhanced light harvesting of Si solar cells via luminescent down-shifting using $YVO_4:Bi^{3+}$, Eu^{3+} nanophosphors

C.K. Huang[1], Y.C. Chen[1], W.B. Hung[1], T.M. Chen[1], K.W. Sun[1]* and W.-L. Chang[2]

[1] Department of Applied Chemistry, National Chiao Tung University, Hsinchu, Taiwan
[2] Green Energy & Environment Research Labs (GEL), Industrial Technology Research Institute (ITRI), Hsinchu, Taiwan

ABSTRACT

The colloids of YVO_4 nanoparticles on microtextured Si surface are demonstrated to have promising potential for efficient solar spectrum utilization in crystalline Si solar cells. The solar cells showed an enhancement of 4% in short-circuit current density and approximately 0.7% in power conversion efficiency when coated with YVO_4 nanoparticles. The properties of cells integrated with YVO_4 nanoparticles were characterized to identify the role of YVO_4 in improved light harvesting. The current experiments conclude that the colloids of YVO_4 nanoparticles not only act as luminescent down-shifting centers in the ultraviolet region but also serve as an antireflection coating for enhancing the light absorption in the measured spectral regime.

KEYWORDS

nanophosphor; luminescence down-shifting; antireflection; spin coating

***Correspondence**

K.W. Sun, Department of Applied Chemistry, National Chiao Tung University, Hsinchu, Taiwan.
E-mail: kwsun@mail.nctu.edu.tw

Received 1 December 2011; Revised 23 January 2011; Accepted 30 March 2012

1. INTRODUCTION

The theoretical maximum efficiency of a single-junction solar cell is specified using the Shockley–Queisser limit [1], which defines the maximal output power as a function of the bandgap of a solar cell. Limitations set on the maximum efficiency of the cells are caused by the following two primary loss mechanisms in solar cells: (i) sub-bandgap-energy photon loss, where the energy of the photons is not enough to excite the active layer and generate electron–hole pairs [2], and (ii) thermalization of charge carriers caused by the absorption of high-energy photons with energies larger than the bandgap of the solar cell. These fundamental losses directly lead to an efficiency limit of approximately 30% for all single-junction cells under nonconcentrated Air Mass 1.5 (AM 1.5) illumination [1].

More efficient utilization of the short wavelength part of the solar spectrum can be achieved by improving the electronic properties of existing devices, such as using the advanced structure design [3–5]. However, these steps are either difficult to implement or expensive to mass produce. The luminescent down-shifting (LDS) of the incident spectrum is a passive approach that can overcome the limitations mentioned previously. The application of an LDS layer was first demonstrated in the late 1970s to improve the poor spectral response (SR) of solar cells to short wavelength light. The LDS layer absorbs photons, typically in the 300–500 nm range and re-emits them at a longer wavelength, where the photovoltaic (PV) device exhibits a significantly better response [6]. The LDS layer can help in harvesting full solar energy by expanding the operating spectral range towards the ultraviolet (UV) range. Detailed reviews of the progress in this area can be found in [6].

Luminescent species have been investigated for LDS. They can be separated into three main categories, namely the quantum dots (QDs) [7–9], organic dyes [10], and rare-earth ions/complexes [11]. These luminescent species provide enhancements in the short-λ response of PV devices. Thus, more electron–hole pairs can be created per incident photon, and a higher short-circuit current (I_{SC}) can be generated. The LDS material was reported to improve the efficiency of dye-sensitized solar cells by 23.3% [12]. More recently, the commercial fabrication procedure of the multicrystalline Si cell has achieved 40% external quantum efficiency (EQE) at wavelengths of less than 400 nm by combining luminescent organic dyes [10].

Most previous research presented the good performance of LDS in a planar luminescent sheet positioned on top of the PV cells. However, the introduction of an LDS layer in a PV module also creates additional interactions with light that results in extra loss mechanisms [6]. The major obstacles in the development of LDS method, such as photostability of organic luminescent molecules [13], low quantum efficiency of luminescent species [13], and absorption of the host materials [14], had been the inadequacy of the properties of the available materials.

YVO_4 is a widely used optical material with many good features, including excellent thermal efficiency and high luminescent quantum efficiency [15–17]. The trivalent lanthanide ions (Ln^{3+}) with abundant energy levels arising from the $4f^n$ inner shell configuration offer the ability of photon management when doped in the YVO_4 [17], and thus, they are well suited for spectral conversion in solar cells. The experimental bandgap for YVO_4 is 3.8 eV, whereas the replacement of Y^{3+} ions with Bi^{3+} ions could result in a significant reduction in the bandgap [18]. The Bi^{3+} ion was proven to be an excellent sensitizer for Ln^{3+} ions in a YVO_4 host not only with enhanced luminescent intensity but also with broadened excitation spectrum [19]. Therefore, YVO_4:Bi^{3+}, Eu^{3+} phosphors are promising UV-absorbing spectral converters for solar cells because they possess broadband absorption in the whole UV region of 250 to 400 nm and they allow to the emission of intense visible lights.

The current study demonstrates the increase in conversion efficiency of Si solar cells by incorporating rare-earth element-doped YVO_4 luminescent nanoparticles directly (without host materials) onto the textured surface of the devices. The current study aims to investigate the quantum efficiency enhancement associated with light harvesting and the energy transfer properties of the YVO_4:Bi^{3+}, Eu^{3+} nanophosphors.

2. EXPERIMENTAL

The crystalline Si (c-Si) solar cell device used in the current experiment was manufactured following the procedures reported in [20]. Ytterium nitrate hexahydrate [$Y(NO)_3{\cdot}6H_2O$], europium chloride [$EuCl_3$], and polyethylenimine (25 kDa, branched) were purchased from Sigma-Aldrich. Ammonium metavanadate [NH_4VO_3] was obtained from SHOWA (Chemical Co., LTD., Tokyo, Japan). Bismuth nitrate pentahydrate [$Bi(NO)_3.5H_2O$] was supplied by Merck (Whitehouse Station, NJ, USA). All reagents were used as received.

In a typical preparation, the stoichiometry amounts of $Y(NO)_3{\cdot}6H_2O$, $Bi(NO)_3{\cdot}5H_2O$, and $EuCl_3$ were dissolved in a nitric acid aqueous solution. NH_4VO_3 was dissolved in deionized water and was added drop-wise into the aforementioned mixture solution under vigorous stirring. The capping agent, polyethylenimine, was added into the mixture solution heated at 80 °C, and the pH value was adjusted to 6. After being stirred for 1 h, the precursor solution was transferred into 100 ml Teflon-lined autoclave and heated subsequently at 180 °C for 24 h. The obtained precipitate was collected via centrifugation and then washed with ethanol and deionized water several times. After being dried in an oven at 80 °C for 24 h, YVO_4:Bi^{3+}, Eu^{3+} nanophosphors were obtained.

The YVO_4 nanophosphors were first dispersed in deionized water to make a 2.5, 5, 7.5, and 10 mg/ml solutions, respectively. Spin-coating technique was used for nanophosphor deposition. With the use of the solution concentrations of 2.5, 5, 7.5, and 10 mg/ml of the YVO_4 nanophosphors, uniform and perfect light scattering thin films with a thickness of about 100 nm were obtained under properly controlled spin-coating rates. The c-Si cells with and without the nanophosphors were evaluated at room temperature on the basis of the illuminated current density versus voltage (*J–V*) characteristics, EQE, and reflectance. The photocurrent was analyzed using a solar simulator under the Air Mass 1.5 Global (AM 1.5G) illumination condition (100 mW/cm^2, 25 °C). The EQE was measured using an AM 1.5G standard spectrum and an Optosolar simulator (SR-150). The reflectance spectra of the samples were recorded using a UV–visible–near infrared (NIR) spectrophotometer (Hitachi U-4100) for wavelengths ranging from 200 to 1200 nm. X-ray diffraction (XRD) of the samples was measured on a Bruker AXS D8 (Karlsruhe, Germany) advanced automatic diffractometer with Cu Kα radiation. The photoluminescence spectra of the nanophosphors were measured using a Spex Fluorolog-3 Spectrofluorometer (Jobin Yvon Inc., Edison, NJ, USA) equipped with a 450 W Xe light source. The quantum efficiency of the nanophosphors was measured using an integrating sphere, whose inner face was coated with Spectralon equipped with a spectrofluorometer (Horiba Jobin-Yvon Fluorolog 3–22 Tau-3). The corresponding optical absorbance (φ) and quantum efficiency (η) were calculated using the equations from [21].

3. RESULTS AND DISCUSSION

In Figure 1(a), the scanning electron microscope (SEM) image of the YVO_4 nanophosphors shows that the nanophosphors had a nearly spherical shape with an average diameter of approximately 20 nm. The size distribution of the nanophosphors is further confirmed by the dynamic light scattering measurements, as given in Figure 1 (b). The XRD pattern of the YVO_4 nanophosphors is also displayed in the inset of Figure 1(a). The peaks at the 2θvalues of 18.83°, 33.6°, 25.02°, and 49.82° can be indexed to the (101), (112), (200), and (312) planes of YVO_4, respectively, which match well with the standard diffraction data of YVO_4 (ICSD no. 78074). The nominal chemical composition of the nanophosphors is $Y_{0.7}Bi_{0.15}Eu_{0.15}VO_4$ from the stoichiometry amounts of $Y(NO)_3{\cdot}6H_2O$, $Bi(NO)_3{\cdot}5H_2O$, $EuCl_3$, and NH_4VO_3 used in the preparation. This composition is also supported from the results of XRD (as shown in the inset of Figure 1(a)) and energy dispersive spectroscopy (as shown in Figure 2(a)). We have also fabricated and

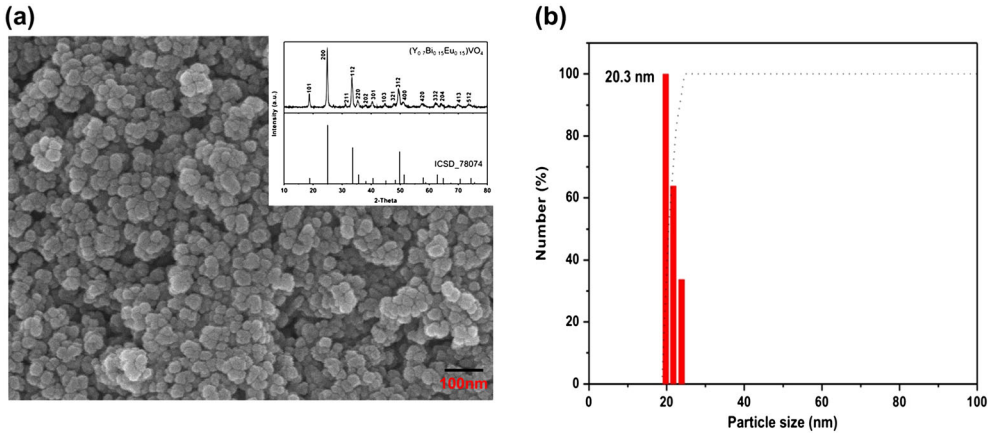

Figure 1. (a) Scanning electron microscope image of YVO_4 nanophosphors with an average diameter of ~20 nm. Inset shows the X-ray diffraction pattern of YVO_4 nanoparticles. (b) Size distributions of nanophosphors determined by dynamic light scattering measurements.

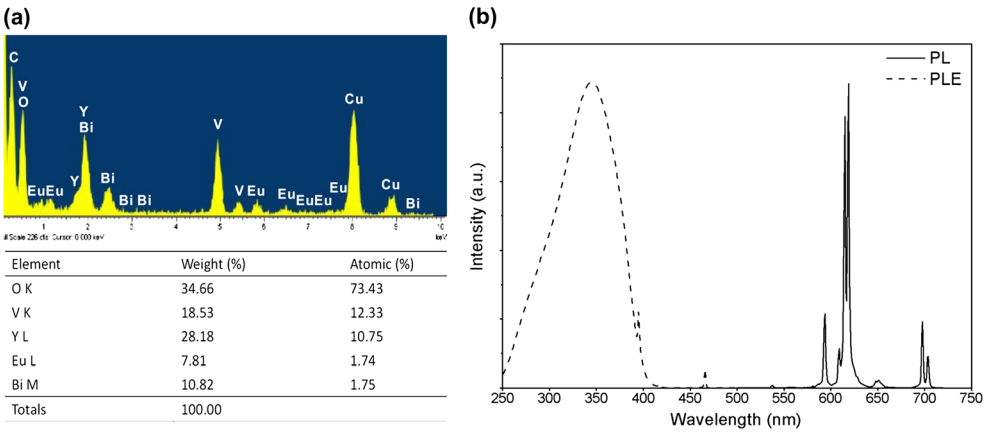

Element	Weight (%)	Atomic (%)
O K	34.66	73.43
V K	18.53	12.33
Y L	28.18	10.75
Eu L	7.81	1.74
Bi M	10.82	1.75
Totals	100.00	

Figure 2. (a) Energy dispersive spectrum of YVO_4:Bi^{3+}, Eu^{3+}. (b) Photoluminescence excitation (PLE; dash curve) and photoluminescence excitation (PL; solid curve) spectra of YVO_4 NPs in toluene. The photoluminescence excitation spectrum was measured at a fixed detection wavelength of 619 nm. For the photoluminescence excitation spectrum, samples were excited by a light beam at 350 nm.

tested YVO_4 with different Bi^{3+} and Eu^{3+} compositions. However, nanophosphors with the composition of $Y_{0.7}Bi_{0.15}Eu_{0.15}VO_4$ give the best down-conversion efficiency of approximately 15% (data not shown here). Therefore, nanophosphors with this particular composition were used throughout the entire experiments.

Figure 2(b) shows the photoluminescence excitation (PLE) and fluorescence spectra of the YVO_4 nanophosphors in toluene. The fluorescence spectrum showed a major emission at 619 nm when the particles were excited at a wavelength of 350 nm. The PLE spectrum was measured at a fixed detection wavelength of 619 nm. The spectrum shows the broad resonance expansion from 250 to 410 nm with a peak centered at around 352 nm, indicating that the YVO_4 nanophosphors exhibit the photon down-shifting property by absorbing of UV photons and converting them into visible with a high luminescent quantum efficiency of approximately 15%.

The SEM image at low magnification shows the as-prepared YVO_4 nanophosphor colloids (with a concentration of 5 mg/ml) deposited directly on the c-Si cell textured surface with a thickness of 120 to 150 nm, as shown in Figure 3. Figure 4 shows the schematic of the proposed structure design. Given that most of incident UV radiations produce electron–hole pairs near the device surface, the photo-generated carriers disappear easily through their recombination with surface defects, which can lead to inferior cell efficiency. However, with the presence of the YVO_4 nanophosphors on the front side, more photons can be absorbed closer to the depletion region once the UV photons are luminescent down-shifted to the visible. The built-in electric field will automatically separate the photo-generated electron–hole pairs and enhance the PV effect.

The electrical characterizations on solar cells coated with YVO_4 nanophosphors with different densities were

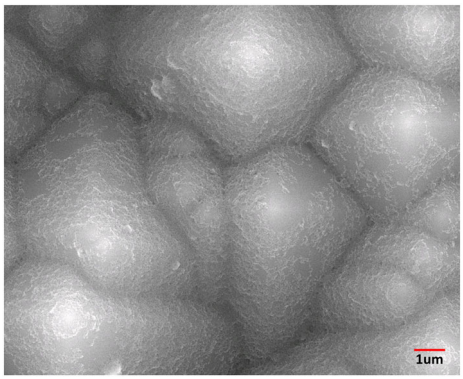

Figure 3. Scanning electron microscope image at low magnification of the YVO_4 nanophosphor layer on the textured solar cell surface at a concentration of 5 mg/ml.

performed by varying the concentrations of YVO_4 nanophosphors solution from 2.5 to 10 mg/ml. Figure 5 shows the results of the characterizations, which helped in obtaining the optimal particle density of YVO_4 nanophosphors for a better power conversion efficiency. Figure 5 shows that the best overall power conversion efficiency η increased from 16.6% to 17.3%. The increases in conversion efficiencies of the solar cells with the YVO_4 nanophosphors were 0.3%, 0.7%, and negligible change for the 2.5, 5, and 7.5 mg/ml particle densities, respectively, at a fixed dose volume of 300 µl. The highest efficiency increase of 0.7% was achieved when the solar cell surface was covered with YVO_4 nanophosphors using a concentration of 5 mg/ml. As shown in Figure 5, the enhancement factors began to drop when the solution concentration exceeded 5 mg/ml, and eventually, the cell efficiency started to deteriorate when the particle densities were higher than 7.5 mg/ml. This phenomenon was attributed to the substantial absorption in the UV region by YVO_4 nanophosphors, which eventually led to the considerable loss of the original UV transmittance towards the cell.

Figure 6 shows the changes in the reflectance of the solar cells with different YVO_4 particle densities. Noted that the reflectance in the visible and NIR was slightly reduced with the presence of nanophosphors. The most significant change in the reflectance took place in the spectral region around 320 nm mostly because of the absorption

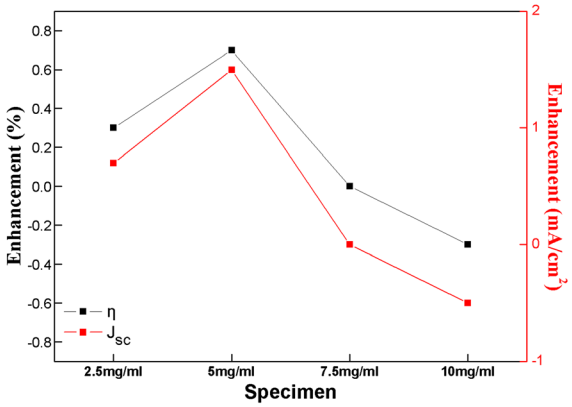

Figure 5. Gains in conversion efficiency and current density of c-Si solar cells after optimizing the spin-coating recipe and areal densities of YVO_4 nanophosphors.

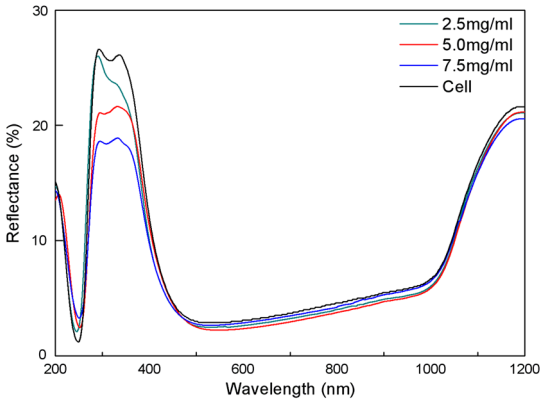

Figure 6. Reflectance at maximum performance of solar cells integrated with different densities of YVO_4 nanophosphors with solution concentrations of 2.5, 5, and 7.5 mg/ml. The spectrum of an untreated device is also displayed in parallel for comparison.

by YVO_4 nanoparticles. However, at the optimal nanoparticle density of 5 mg/ml, the reflectance in the UV only dropped by less than 4% in comparison with the cell without nanophosphors. This indicated that EQE of the original cell in the UV was not affected by the presence of YVO_4 nanoparticles. Unlike in the case where Si QDs were used as the frequency down-shifting material [7], due to significant absorption by the spin-coated Si QDs layer in the

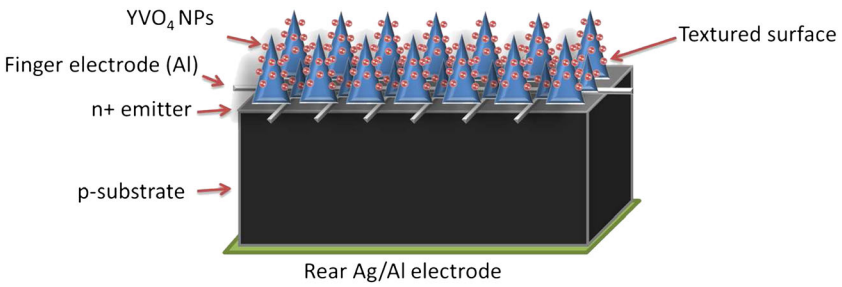

Figure 4. Schematic of textured cell structures covered with YVO_4 nanophosphors.

DOI: 10.1002/pip

UV, a down-shifting efficiency of more than 40% was required to enhance solar cell efficiency. As in our case, as long as the particle density is kept at its optimal value, the solar cell efficiency can be further improved as the down-shifting efficiency of YVO_4 increases.

External quantum efficiency measurements were performed, in which a xenon light source was used as the illumination source, to understand the underlying mechanisms for the enhanced cell efficiency. The EQE of the c-Si solar cells coated with different densities of YVO_4 nanophosphors were measured relative to the cells without nanophosphors treatment (Figure 7). The presence of the YVO_4 nanophosphors provides a clearly visible EQE enhancement in the UV, indicating that the increase in photocurrent is mostly due to the enhanced absorption of UV by the YVO_4 nanophosphors. In the visible and NIR region, because there is no PLE signal from YVO_4, luminescence down-shifting cannot entirely account for the enhancement of EQE. Therefore, the scattering provided by the nanophosphors is believed to be essential for coupling and partially trapping light in substrate radiation modes [7,9,20,22], which also leads to the slight increase in quantum efficiency. There are two possible mechanisms responsible for the enhancement of EQE for SR above 450 nm. First, the scattering of incident light by the porous nanophosphor layer enabled the improved transmission of photons into the semiconductor active layers and the coupling of normally incident photons into the lateral, resulting in the increased photon absorption, photocurrent generation, and power conversion efficiency of the solar cells [20,22]. Second, considering a simple effective medium approximation of the nanophosphors on the Si_3N_4 surface, a YVO_4 nanophosphors layer with an average refractive index of $n \approx 1.9$ provided an improved index matching and acted as a good antireflection coating when sandwiched between the Si_3N_4 ($n \approx 2.0$) and air ($n \approx 1$). The SEM images of the solar cell coated with the YVO_4 at high magnification, as shown in Figure 8, revealed the porous nanostructures of the spin-coated nanophosphor layer. Enhancement of solar cell efficiency induced by surface porosity was reported in QDs/nanoparticles coated solar cells [7,9]. However, significant improvements in both reflectance and EQE can only be achieved with the proper areal coverage of nanophosphors.

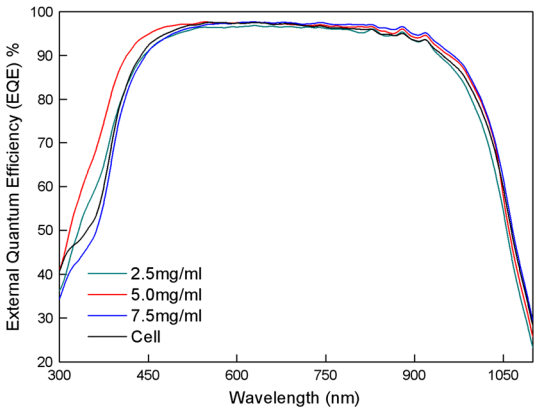

Figure 7. External quantum efficiency at maximum performance measured under AM 1.5G illumination for solar cells integrated with different densities of YVO_4 nanophosphors.

The EQE measurements are in agreement with the reflectance results, where the cell response improved in the wavelength ranges of UV and NIR because of the LDS and scattering of the YVO_4 nanophosphors. In the best case, the EQE enhancement ratio of the c-Si solar cells with a concentration of 5 mg/ml of YVO_4 nanophosphors was over 28% in the UV regions, as shown in Figure 9. Compared with the PLE spectrum of YVO_4 nanophosphors shown in Figure 2(b), the resonance peak in the PLE spectrum was coincident with the position of the maximum enhancement in EQE at approximately 360 nm. Therefore, the enhanced SR below 425 nm is indeed attributed to the photon frequency down-shifting.

Figure 10 shows the current–voltage (J–V) characteristics of the solar cell at maximum enhancement. The performance of the cell without YVO_4 nanophosphors was also presented in parallel for comparison. The short-circuit current density (J_{sc}), open-circuit voltage (V_{oc}), fill factor,

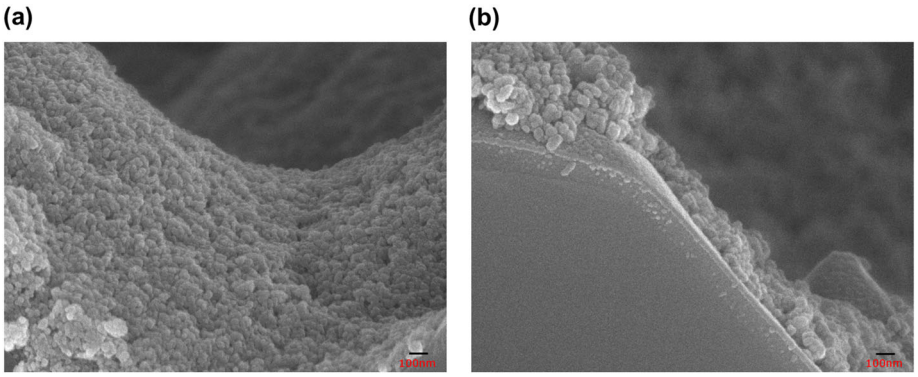

Figure 8. Scanning electron microscope images of (a) plane view and (b) side view of the YVO_4 nanophosphor layer at high magnification on the textured solar cell surface at a concentration of 5 mg/ml.

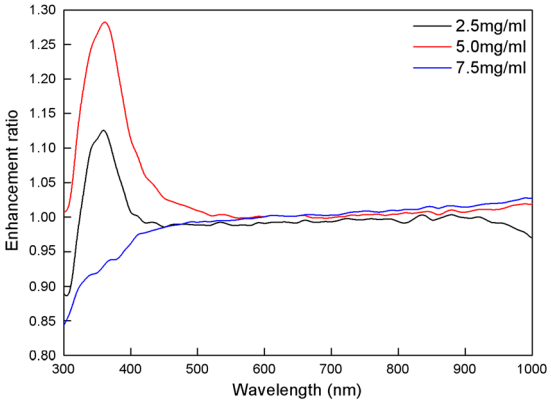

Figure 9. Enhancement ratio of external quantum efficiency as a function of wavelength at different YVO_4 nanophosphor densities.

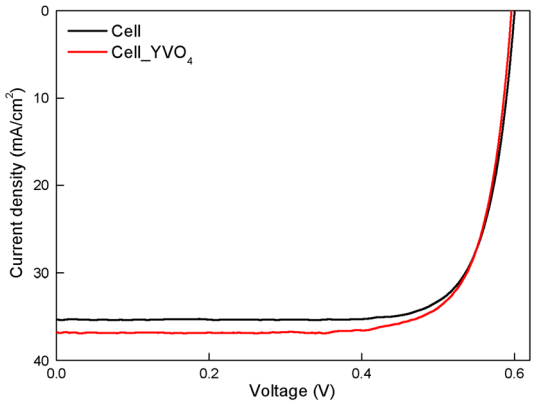

Figure 10. *J–V* characteristics of the optimized solar cells integrated with 5 mg/ml of the YVO_4 nanophosphors. Result from a device without YVO_4 treatment is displayed for comparison.

and conversion efficiency for the experiment cells were 36.8 mA/cm^2, 0.59 V, 0.77, and 17.3%, respectively. The values for the reference cells were 35.3 mA/cm^2, 0.59 V, 0.78, and 16.6%, respectively. V_{oc} and fill factor remained almost unaffected as J_{sc} increased from 35.3 to 36.8 mA/cm^2 with the integrated YVO_4 nanophosphors. Therefore, the enhancement in cell efficiency can indeed be attributed to the increase in photocurrent and light absorption. This agrees with the observation in the improved reflectance shown in Figure 6.

YVO_4 nanophosphors, as LDS materials with a wide UV absorption band and a high luminescent quantum efficiency (~15%), are a good alternative to achieve an enhanced solar cell performance at a low cost, easy to manufacture, and environmentally friendly. The YVO_4 nanophosphor suffers no oxidation problem, and therefore, it gives a better stability of efficiency enhancement over solar cells coated with semiconductor QDs/nanoparticles, such as Si QDs. In addition to the novel property of LDS shown in the current report, the surface roughness of the cells increased after the deposition of the YVO_4 nanophosphors, which reduced the sensitivity of the devices on the incidence light angles. As a result, photons that reached the YVO_4–air interface had more chances of being trapped in the solar cell and were then converted to photocurrents, especially at dawn and sunset (large incident angles) [23].

4. CONCLUSION

In summary, YVO_4 nanophosphors were directly integrated into the textured solar cell surface without host materials. The proposed hybrid system was shown to significantly enhance power conversion efficiency using the AM 1.5 illumination. The underlying mechanisms of the observed enhancement are attributed to LDS, as well as to index matching and light trapping. Unprecedented device performance can be expected with further improvement in LDS quantum yield and florescence bandwidth in the visible. This approach is believed to be able to find promising applications in other types of solar cells and opens new possible schemes to exploit nanophosphors for energy devices.

ACKNOWLEDGEMENTS

The current work was partially supported by the Bureau of Energy in Taiwan and National Science Council of the Republic of China under Grant No. NSC 99-2119-M-009-004-MY3.

REFERENCES

1. Shockley W, Queisser HJ. Detailed balance limit of efficiency of p–n junction solar cells. *Journal of Applied Physics* 1961; **32**: 510–519.
2. Goldschmidt SFJC, Löper P, Krmer KW, Biner D, Hermle M, Glunz SW. Proc. 25th Eur. Photovoltaic Solar Energy Conf. and Exhibition (25th EU PVSEC) Goldschmidtyr, 2010. P.229.10.4229/25thEUPVSEC2010-1CO.6.5.
3. Bedair SM, Lamorte MF, Hauser JR. A two-junction cascade solar-cell structure. *Applied Physics Letters* 1979; **34**: 38. DOI: 10.1063/1.90576
4. Taguchi M, Kawamoto K, Tsuge S, Baba T, Sakata H, Morizane M, Uchihashi K, Nakamura N, Kiyama S, Oota O. HIT (TM) cells — high-efficiency crystalline Si cells with novel structure. *Progress in Photovoltaics* 2000; **8**: 503–513.
5. Luque A, Marti A. Increasing the efficiency of ideal solar cells by photon induced transitions at intermediate levels. *Physical Review Letters* 1997; **78**: 5014–5017.

6. Klampaftis E, Ross D, McIntosh KR, Richards BS. Enhancing the performance of solar cells via luminescent down-shifting of the incident spectrum: a review. *Solar Energy Materials and Solar Cells* 2009; **93**: 1182–1194. DOI: 10.1016/j.solmat.2009.02.020
7. Pi XD, Li Q, Li DS, Yang DR. Spin-coating silicon-quantum-dot ink to improve solar cell efficiency. *Solar Energy Materials and Solar Cells* 2011; **95**: 2941–2945.
8. Cheng Z, Su F, Pan L, Cao M, Sun Z. CdS quantum dot-embedded silica film as luminescent down-shifting layer for crystalline Si solar cells. *Journal of Alloys and Compounds* 2010; **494**: L7–L10. DOI: 10.1016/j.jallcom.2010.01.047
9. Huang CY, Wang DY, Wang CH, Chen YT, Wang YT, Jiang YT, Yang YJ, Chen CC, Chen Y-F. Efficient light harvesting by photon downconversion and light trapping in hybrid ZnS nanoparticles/Si nanotips solar cells. *ACS Nano* 2010; **4**: 5849–5854.
10. McIntosh KR, Lau G, Cotsell JN, Hanton K, Bätzner DL, Bettiol F, Richards BS. Increase in external quantum efficiency of encapsulated silicon solar cells from a luminescent down-shifting layer. *Progress in Photovoltaics: Research and Applications* 2009; **17**: 191–197. DOI: 10.1002/pip.867
11. Marchionna S, Meinardi F, Acciarri M, Binetti S, Papagni A, Pizzini S, Malatesta V, Tubino R. Photovoltaic quantum efficiency enhancement by light harvesting of organo-lanthanide complexes. *Journal of Luminescence* 2006; **118**: 325–329. DOI: 10.1016/j.jlumin.2005.09.010
12. Liu J, Yao Q, Li Y. Effects of downconversion luminescent film in dye-sensitized solar cells. *Applied Physics Letters* 2006; **88**: 173119. DOI: 10.1063/1.2198825
13. Hovel HJ, Hodgson RT, Woodall JM. The effect of fluorescent wavelength shifting on solar cell spectral response. *Solar Energy Materials* 1979; **2**: 19–29.
14. van Sark WGJHM, Meijerink A, Schropp REI, van Roosmalen JAM, Lysen EH. Enhancing solar cell efficiency by using spectral converters. *Solar Energy Materials and Solar Cells* 2005; **87**: 395–409. DOI: 10.1016/j.solmat.2004.07.055
15. Xu Z, Kang X, Li C, Hou Z, Zhang C, Yang D, Li G, Lin J. Ln3 + (Ln = Eu, Dy, Sm, and Er) ion-doped YVO4 nano/microcrystals with multiform morphologies: hydrothermal synthesis, growing mechanism, and luminescent properties. *Inorganic Chemistry* 2010; **49**: 6706–6715. DOI: 10.1021/ic100953m
16. Xie L, Song H, Wang Y, Xu W, Bai X, Dong B. Influence of concentration effect and Au coating on photoluminescence properties of YVO4:Eu3 nanoparticle colloids. *Journal of Physical Chemistry C* 2010; **114**: 9975–9980.
17. Li LP, Zhao ML, Tong WM, Guan XF, Li GS, Yang LS. Preparation of cereal-like YVO(4):Ln(3+) (Ln = Sm, Eu, Tb, Dy) for high quantum efficiency photoluminescence. *Nanotechnology* 2010; **21**: 195601.
18. Dolgos MR, Paraskos AM, Stoltzfus MW, Yarnell SC, Woodward PM. The electronic structures of vanadate salts: cation substitution as a tool for band gap manipulation. *Journal of Solid State Chemistry* 2009; **182**: 1964–1971. DOI: 10.1016/j.jssc.2009.04.032
19. Natarajan V, Dhobale A, Lu C. Preparation and characterization of tunable YVO4: Bi3+, Sm3+ phosphors. *Journal of Luminescence* 2009; **129**: 290–293. DOI: 10.1016/j.jlumin.2008.10.001
20. Huang CK, Lin HH, Chen JY, Sun KW, Chang WL. Efficiency enhancement of the poly-silicon solar cell using self-assembled dielectric nanoparticles. *Solar Energy Materials and Solar Cells* 2011; **95**: 2540–2544. DOI: 10.1016/j.solmat.2011.03.006
21. de Mello JC, Wittmann HF, Friend RH. An improved experimental determination of external photoluminescence quantum efficiency. *Advanced Materials* 1997; **9**: 230–232.
22. Derkacs D, Chen WV, Matheu PM, Lim SH, Yu PKL, Yu ET. Nanoparticle-induced light scattering for improved performance of quantum-well solar cells. *Applied Physics Letters* 2008; **93**: 091107. DOI: 10.1063/1.2973988
23. Chen C-P, Lin P-H, Chen L-Y, Ke M-Y, Cheng Y-W, Huang J. Nanoparticle-coated n-ZnO/p-Si photodiodes with improved photoresponsivities and acceptance angles for potential solar cell applications. *Nanotechnology* 2009; **20**: 245204. DOI: 10.1088/0957-4484/20/24/245204